Research articles

Modeling of multi-axial stress dependent iron losses in electrical steel sheets

U. Aydin[a,b,*], P. Rasilo[b], F. Martin[a], A. Belahcen[a], L. Daniel[c], A. Arkkio[a]

[a] Department of Electrical Engineering and Automation, Aalto University, FI-00076 Espoo, Finland
[b] Unit of Electrical Engineering, Tampere University, FI-33720 Tampere, Finland
[c] Group of Electrical Engineering – Paris, UMR CNRS 8507, CentraleSupélec, Univ. Paris-Sud, Université Paris-Saclay, Sorbonne Université, 3 & 11 rue Joliot-Curie, Plateau de Moulon 91192 Gif-sur-Yvette Cedex, France

ABSTRACT

Modeling the effect of multi-axial mechanical stress on the iron losses of an M400-50A grade non-oriented electrical steel sheet is studied. By utilizing the statistical loss theory, the total measured iron losses are first segregated to hysteresis, classical eddy current and excess losses. Then, the stress dependency of the excess losses is modeled by correlating them to the hysteresis losses under multi-axial stress. This correlation, coupled with a magneto-elastic invariant based loss model, can be used to predict the iron loss evolution with reasonable accuracy under multi-axial stress when only iron loss data under no applied stress at various excitation frequencies and under only two uniaxial stress levels at quasi-static excitation are available. Consequently, this approach significantly reduces the required measurement data for estimating the iron losses under multi-axial stress.

1. Introduction

Magnetic properties of electrical steel sheets are known to be mechanical stress dependent. During the manufacturing of electrical machine cores, electrical steel sheets are punched, stacked, welded and shrink fitted to the frame. These processes together with machine operation conditions cause multi-axial stresses on the core material [1–5]. The performance of the electrical machines are affected significantly due to these multi-axial stresses [6–8,5]. Therefore, in order to be able to design more efficient devices and analyse existing ones with better accuracy, the dependency of the core losses on the multi-axial stresses should be studied.

The previous research commonly studies the effect of uniaxial stress on the iron loss components neglecting the multi-axiality of the stress as it occurs in electrical machines [9–14]. These studies rely on fitting the parameters of statistical loss models to the measured losses under various uniaxial magneto-mechanical loadings. The main conclusion of these studies is that the uniaxial stress has strong influence on both hysteresis and excess losses whereas the classical eddy current losses are stress independent. In [11] an interesting result was reported stating that the excess loss coefficient is proportional to the square root of the hysteresis loss density under uniaxial stress. This result was reached following the conclusion of early work of Bertotti [15] under no applied stress. The hysteresis-excess loss correlation under uniaxial stress allows developing uniaxial stress dependent loss models utilizing

only quasi-static magneto-mechanical measurements. However, whether this correlation holds in the case of multi-axial loading has not been studied.

Few experimental studies were performed in the past to study the multi-axial stress dependency of the iron losses [16–18]. However, these experiments were performed only at single magnetizing frequency which was not sufficient to study the effect of stress on different iron loss components. On the other hand, some recent studies showed that the hysteresis and dynamic losses are affected significantly by the application of multi-axial stresses [19,20]. These studies reports that the effect of multi-axial stress on the iron losses can be much more significant than that of uniaxial stress.

Since performing multi-axial magneto-mechanical measurements is practically a difficult task, models that can be identified only from uniaxial measurements to predict the multi-axial stress dependent iron losses are needed. Such a model based on the equivalent stress principle has been proposed in [19]. Another model was developed in [20] using two magneto-mechanical invariants. Both of these models utilize the statistical loss model of Bertotti [15] and require uniaxial stress dependent iron loss measurements at various magnetizing frequencies to be identified.

In this paper, the validity of the correlation between the hysteresis and excess losses of [11] is tested in the case of multi-axial loading using measurements performed on an M400-50A grade non-oriented electrical steel [20]. Owing to the hysteresis-excess loss correlation and
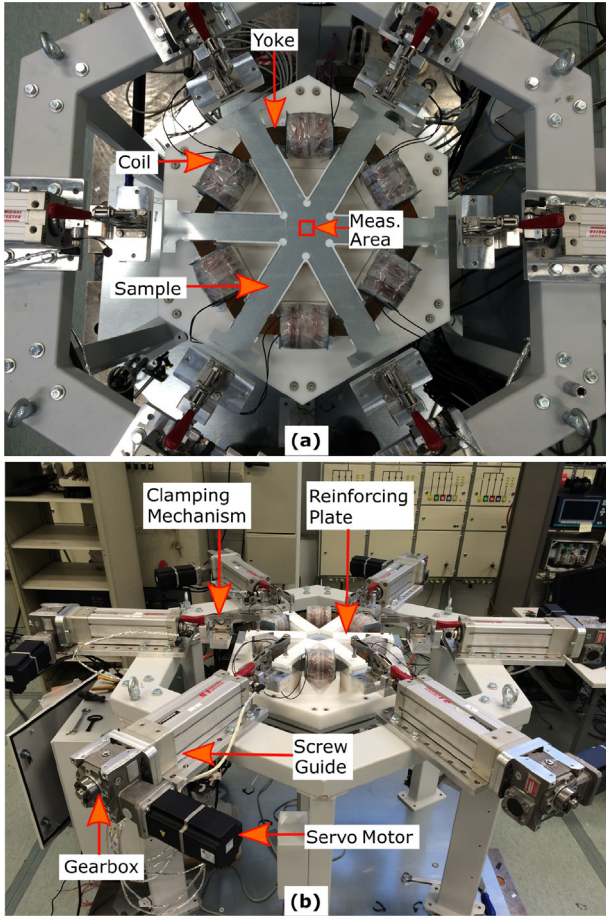

Fig. 1. Single sheet tester device shown (a) from top, (b) as a whole.

magneto-mechanical invariant model, the multi-axial stress dependent iron losses can be predicted with a reasonable accuracy when only iron loss data under no applied stress at various excitation frequencies and under only two uniaxial stress levels at quasi-static excitation are available.

2. Magneto-mechanical measurements

A custom-made single sheet tester device which allows applying arbitrary magneto-mechanical loading on steel sheets was used to perform the magneto-mechanical measurements on a M400-50A non-oriented electrical steel. The flat geometry of electrical steel sheets allows in-plane study of the geometry. Therefore, the stress tensor in the plane of the sheet can be expressed as $\sigma = [\sigma_{xx} \quad \sigma_{yy} \quad \tau_{xy}]^T$. In order to control three components of the stress tensor, controlled stress application along three distinct axes is needed. A six-leg sample geometry as shown in Fig. 1 allows controlling each stress component of σ. One of the most important aspects of magneto-mechanical testing is to obtain homogenous stress and magnetic flux density (B) distribution in the measurement area. The homogeneity of these quantities in the measurement area located at the central region of the sample was ensured during the design stage of the sample geometry with finite element simulations. In a measurement area of 20×20 mm^2 the maximum relative standard deviations of the stress and magnetic flux density were found to be 4.38% and 2.74%, respectively. Mechanical stresses should be applied to each leg pair independently to ensure the homogeneity of stress distribution. A negligible displacement in the central point of the sample is preferred so that six actuators are needed. The actuators driven with servo motors were displaced to apply forces to the sample legs in order to obtain desired stress tensor in the measurement area.

On the other hand, the magnetization system consists of six magnetization coils wound around magnetizing yokes that are placed between each leg of the sample. The sample was magnetized with a controlled 3-phase voltage waveform to obtain sinusoidally alternating magnetic flux density in the measurement area along the rolling direction. Magnetic flux density components along rolling (x) and transverse (y) directions were measured with two search coils placed in the measurement area perpendicular to each other. To measure the magnetic flux strength (H) in the measurement area, a double H-coil was used. The details of the test setup design aspects and control procedures were described in [20,21]. A similar test setup has been developed in [16] using an eight-leg sample which also provides arbitrary stress and magnetization loading possibility. In that setup, the stress application was realized by screws that are driven manually and the magnetization of the sample was done by 2-phase excitation system.

Various stress configurations were studied. These include uniaxial stress along rolling ($\sigma_{uni,x}$) and transverse ($\sigma_{uni,y}$) directions, equibiaxial stress (σ_{equ}) and two cases of pure shear stress which are denoted as shear-I (σ_{sh1}) and shear-II (σ_{sh2}). The servo motors are controlled to apply forces to the sample legs in order to obtain desired stress tensor in the measurement area. The studied magnetization and stress states are expressed as

$$B = [B_p \quad 0 \quad 0]^T, \quad \sigma_{uni,x} = [\sigma \quad 0 \quad 0]^T,$$
$$\sigma_{uni,y} = [0 \quad \sigma \quad 0]^T, \quad \sigma_{equ} = [\sigma \quad \sigma \quad 0]^T, \tag{1}$$

$$\sigma_{sh,I} = [\sigma \quad -\sigma \quad 0]^T, \quad \sigma_{sh,II} = [0 \quad 0 \quad \sigma]^T.$$

The magnitude of σ varies from -30 to $+30$ MPa with 10 MPa intervals. Magnetization curves under the stress states given in (1) were measured when the sample was magnetized along the rolling direction with sinusoidal flux density at amplitude $B_p = 1$ T and at 10 Hz, 30 Hz, 70 Hz, 110 Hz and 150 Hz frequencies. The waveform control of the flux density has been realized by a feedback control algorithm explained in [21]. The relative error between the measured and reference flux density waveforms along x and y directions are expressed as

$$\epsilon_x = \frac{\|B_x - B_{x,ref}\|}{\|B_{x,ref}\|}, \quad \epsilon_y = \frac{\|B_y - B_{y,ref}\|}{\|B_{y,ref}\|}, \tag{2}$$

where B_x, B_y are the measured flux density waveforms and $B_{x,ref}$, $B_{y,ref}$ are the reference flux density waveforms along the x and y directions, and $\|.\|$ denotes root-mean-square. The waveform control is iterated until the convergence criteria $\epsilon_x < 1\%$, $\epsilon_y < 1\%$ are reached. The waveform control does not give satisfactory convergence at magnetizing frequencies lower than 10 Hz. In addition, repeatability of the measurements lower than 10 Hz is poorer due to noisy signals from H-coils. Thus, the lowest frequency limit was set to be 10 Hz. The highest frequency limit was set by respecting to the maximum power output of the voltage amplifier.

Percentage energy loss density variation with respect to the stress free case under these magneto-mechanical loadings in the case of 10 Hz magnetization frequency is shown in Fig. 2. In Fig. 2(a), the variation under uniaxial ($\sigma_{uni,x}$, $\sigma_{uni,y}$) and biaxial (σ_{equ}, $\sigma_{sh,I}$) stress states and in Fig. 2(b) the variations under shear-II stress ($\sigma_{sh,II}$) are given. When uniaxial compression along the magnetization direction is applied, the losses increase significantly. On the other hand, application of tension along the magnetization direction decreases the losses. The effect is opposite when uniaxial stress is applied perpendicular to the magnetization direction. In the case of biaxial loading, shear-I stress when $\sigma_{xx} < 0$ and bicompression state increases the losses. The decrease in losses is observed when shear-I stress with $\sigma_{xx} > 0$ and bitension is applied. The highest increase in the losses is up to 99.6% and it is caused by the application of shear-I stress when $\sigma_{xx} < 0$. On the other hand, in the case of shear-II stress (Fig. 2(b)), increase in the losses is observed in the both cases when $\sigma < 0$ and $\sigma > 0$.
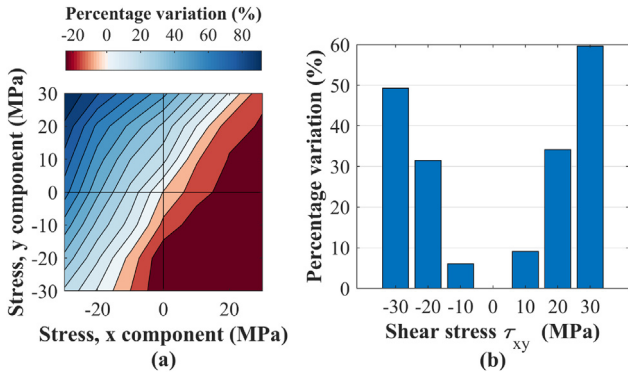
Fig. 2. Measured percentage iron loss variations with respect to stress free case under (a) biaxial and (b) shear-II stress states. Flux density is along rolling (x) direction with 1 T peak induction and 10 Hz magnetizing frequency.

3. Iron loss models

The total iron losses per unit volume, per cycle (w_{tot}) measured under various magnetizing frequencies can be segregated into hysteresis loss (w_{hy}), classical eddy current loss (w_{cl}) and excess loss (w_{ex}) components using the Bertotti loss model [15]. Assuming negligible skin effect and sinusoidal induction, w_{tot} is expressed as

$$w_{tot} = \underbrace{c_{hy}B_p^2}_{w_{hy}} + \underbrace{\frac{\pi^2 d^2 B_p^2 f}{6\rho}}_{w_{cl}} + \underbrace{c_{ex}B_p^{1.5}f^{0.5}}_{w_{ex}} \quad \left[\text{J/m}^3 \right] \tag{3}$$

where ρ, d, B_p and f are resistivity of the material, thickness of the material, peak induction level and the frequency of the field, respectively. The hysteresis and excess loss coefficients c_{hy} and c_{ex} can be identified by fitting (3) to the measured losses. Developing models to include the stress dependency of these coefficients provides a simple way to account for the stress dependency of the iron losses, for instance, as in [11,19,20].

Following the approach of [11], where it was reported that the excess losses are proportional to the square root of the hysteresis losses under uniaxial stress, we introduce Model I. In Model I, stress dependent excess losses are correlated to the hysteresis losses with a single coefficient. Assuming the classical eddy current losses are stress independent [10], Model I allows obtaining the total stress dependent iron losses only with the knowledge of hysteresis loss data under stress utilizing the statistical loss model of Bertotti. Based on this, the total stress dependent energy loss density can be expressed as

$$w_{tot}(\boldsymbol{\sigma}) = \underbrace{c_{hy1}(\boldsymbol{\sigma})B_p^2}_{w_{hy}(\boldsymbol{\sigma})} + \frac{\pi^2 d^2 B_p^2 f}{6\rho} + \underbrace{k\sqrt{w_{hy}(\boldsymbol{\sigma})}\,B_p^{1.5}f^{0.5}}_{w_{ex}(\boldsymbol{\sigma})} \tag{4}$$

where $c_{hy1}(\boldsymbol{\sigma})$ and k are the stress dependent hysteresis loss coefficient and correlation coefficient, respectively. The correlation coefficient k can be identified using only the stress free loss data under various frequencies. The hysteresis loss coefficient $c_{hy1}(\boldsymbol{\sigma})$ is identified by extrapolating the measured stress dependent energy losses per cycle to zero frequency. It is acknowledged that lower-frequency measurements should be performed to improve the accuracy of the loss segregation. However, due to the complex structure of the device, which is required for the multiaxial loading and rotational fields, controlling the flux density in the middle of the sample is challenging, and that good results could not be obtained under 10 Hz as discussed in Section 2. After the identification of k and $c_{hy1}(\boldsymbol{\sigma})$, the stress dependent iron losses at higher frequencies can be obtained with (4). It is worth mentioning that the stress might have indirect effect on the classical eddy current losses since the application of stress affects the skin depth through
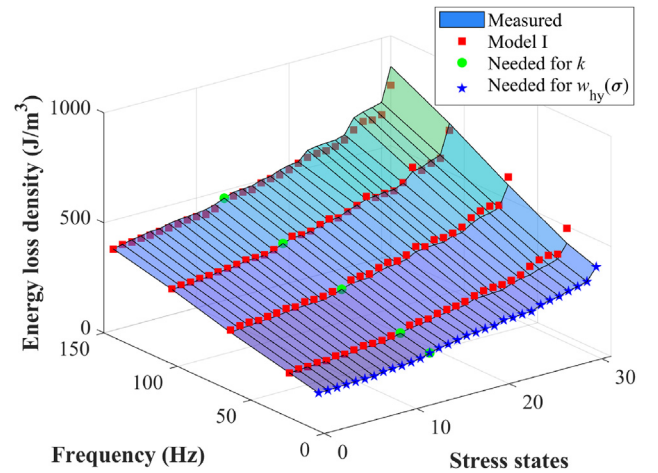

Fig. 3. Measured and modeled total energy loss densities with Model I for each stress and magnetization state. The peak induction is 1 T for all the cases. The losses are sorted as ascending.

permeability. In order to consider the skin depth variation under stress, coupled magneto-mechanical behavior of the material should be modeled. In addition, the thickness of the lamination might also change considerably under high levels of stress, especially beyond the elastic limits. However, under the studied frequency and stress levels both the skin effect and the change in thickness are negligible. Moreover, elastic stress has negligible effect on the resistivity of the material [9,10]. Thus, the classical eddy current losses are assumed to be unaffected by the stress. It is worth noting that under plastic deformation, resistivity varies considerably [22].

In [11] it was shown that the hysteresis-excess loss correlation with a single coefficient is valid under uniaxial loading applied parallel to the field direction, but multiaxial loading was not considered. In order to test the validity of Model I in the case of multi-axial loading, first the parameter k is identified by fitting Model I to the measured total losses at all the studied frequencies and under no applied stress (green markers in Fig. 3). After the identification of k, it is now possible to use (4) and low-frequency loss measurements under multiaxial stress to predict the multiaxial stress dependent losses at higher frequencies. This was done by plugging k to (4) and fitting the expression to the measured total losses at 10 Hz and under all the studied stress configurations given in (1) (blue markers in Fig. 3). The predicted results, shown by the red markers in Fig. 3, correspond relatively well to the measured ones. The relative error

$$\epsilon = \frac{\|w_{sim} - w_{tot}\|}{\|w_{tot}\|} \tag{5}$$

between the measured (w_{tot}) and modeled (w_{sim}) losses is 4.51%. Thus, it is concluded that the hysteresis-excess loss correlation in the case of multi-axial loading is valid.

Although Model I successfully predicts the total losses under multiaxial stress for higher frequencies than it is identified with, in addition to stress free measurements under various frequencies, it still requires low-frequency iron loss data under multi-axial stress for identification of $c_{hy1}(\boldsymbol{\sigma})$. This requirement can be reduced by benefiting the approach given in [20] (Model II). Model II is defined to introduce the stress dependency of the hysteresis loss coefficient based on the magneto-elastic invariants which are given by

$$I_5 = \boldsymbol{b}\cdot(\boldsymbol{sb}), \qquad I_6 = \boldsymbol{b}\cdot(\boldsymbol{s}^2\boldsymbol{b}). \tag{6}$$

Here, $\boldsymbol{b}$ is the direction vector of the flux density and $\boldsymbol{s}$ is the deviatoric part of the applied stress tensor $\boldsymbol{\sigma}$ which is given by $\boldsymbol{s} = \boldsymbol{\sigma} - \frac{1}{3}(\text{tr}\boldsymbol{\sigma})\boldsymbol{I}$. Here, $\boldsymbol{I}$ is the second-order identity tensor. More details about the magneto-mechanical invariants can be found in [23]. Based on I_5 and I_6,
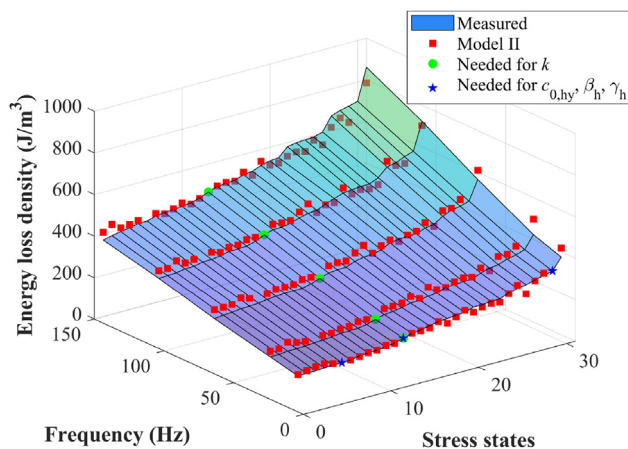
Fig. 4. Measured and modeled total energy loss densities with Model II for each stress and magnetization state. The peak induction is 1 T for all the cases. The losses are sorted as ascending.

the hysteresis loss coefficient c_{hy2} is expressed as

$$c_{hy2}(I_5, I_6) = c_{0,hy} + \beta_h I_5 + \gamma_h I_6 \qquad (7)$$

where $c_{0,hy}$ is the loss coefficients under no applied stress, β_h and γ_h are fitting parameters to be determined. Only two iron loss measurements under uniaxial stress applied parallel to magnetization direction ($\sigma_{uni,x}$) at low magnetizing frequency are sufficient to identify these parameters. After the identification, the multi-axial stress dependent hysteresis losses $w_{hy2}(\sigma)$ can be predicted as

$$w_{hy2}(\sigma) = c_{hy2}(I_5, I_6)B_p^2. \qquad (8)$$

Combining Model I and II allows predicting the multi-axial stress dependent iron losses when only stress free loss measurements at various frequencies and two uniaxial stress dependent measurements at low frequency are available. The procedure is following:

1. Identify k of Model I by fitting (4) to the stress free iron losses at various frequencies (green markers in Fig. 4).
2. Substitute k and $c_{hy2}(I_5, I_6)$ into (4) to obtain the expression

$$w_{tot}(\sigma) = \underbrace{c_{hy2}(I_5, I_6)B_p^2}_{w_{hy2}(\sigma)} + \frac{\pi^2 d^2 B_p^2 f}{6\rho} + k\sqrt{w_{hy2}(\sigma)}\, B_p^{1.5} f^{0.5}, \qquad (9)$$

   and fit the expression to the total losses measured at 10 Hz excitation frequency and under two different uniaxial stresses applied parallel to the flux direction (blue markers in Fig. 4) for identifying $c_{0,hy}$, β_h, and γ_h of $c_{hy2}(I_5, I_6)$. In this paper, for the stress dependent losses, the loss data under uniaxial compression (-30 MPa) and tension ($+30$ MPa) are used.
3. After the parameter identification, calculate the iron losses under multiaxial magneto-mechanical loadings by (9).

Using the above procedure, the losses are modeled under all the measured magneto-mechanical loadings which include the stress states given in (1) and all the measured frequency range. The comparison of the measured and predicted losses are shown in Fig. 4. Although some local variations between the modeled and measured results exist, the overall behavior is modeled with reasonable accuracy. The relative error between the measured and modeled losses is 6.15% which is calculated using (5).

It is worth noting that, here the coefficient c_{hy2} is identified only at single peak induction B_p. The values of β_h and γ_h vary as a function of B_p, since stress affects the losses differently under different inductions. In addition, the stress-free hysteresis loss coefficient $c_{0,hy}$ may vary as a function of B_p, if the B_p^2-dependency of the hysteresis losses in (8) is not

exactly valid. In order to study the effect of stress on the iron losses under different inductions, c_{hy2} can be identified for different inductions following the presented approach.

4. Conclusion

Modeling the multi-axial stress dependency of the iron losses was studied. The correlation of the excess losses to the hysteresis losses was shown to be valid in the case of multi-axial loadings. Thus, in addition to stress free measurements under various frequency, only low-frequency measurements under multi-axial stress are sufficient to model the iron losses at higher frequencies. However, this approach is valid in the frequency range where the skin effect is negligible. Although, this correlation reduces the number of required measurements to obtain the multi-axial stress dependent iron losses at higher frequencies, it still requires complex multi-axial measurements which are difficult to perform.

The requirement of the multi-axial stress dependent loss data was reduced by coupling a predictive loss model based on magneto-elastic invariants with the hysteresis-excess loss correlation. This approach proved to predict the iron loss evolution under multi-axial stress with reasonable accuracy when only stress free loss measurements under various excitation frequencies and under two uniaxial stress levels at low excitation frequency are used for parameter identification. In fact, the requirement for the stress free loss data under several excitation frequencies, that are needed to identify the hysteresis-excess loss correlation parameter, can further be reduced to stress free loss measurements under only two different frequencies. However, in this case the measurement errors can have significant effect on the result of parameter fitting, which can cause large errors at the loss predictions. Thus, it is preferable to use measurements under several magnetizing frequencies for identifying hysteresis-excess loss correlation parameter.

CRediT authorship contribution statement

U. Aydin: Conceptualization, Methodology, Software, Validation, Investigation, Visualization, Writing - original draft. **P. Rasilo:** Conceptualization, Software, Visualization, Writing - review & editing. **F. Martin:** Software. **A. Belahcen:** Supervision, Writing - review & editing. **L. Daniel:** Conceptualization, Writing - review & editing. **A. Arkkio:** Funding acquisition, Writing - review & editing.

Declaration of Competing Interest

The authors declare that they have no known competing financial interests or personal relationships that could have appeared to influence the work reported in this paper.

Acknowledgment

References

[1] Y. Kai, Y. Tsuchida, T. Todaka, M. Enokizono, Evaluation of local residual stress distribution of stator core in rotating machine, EEJ Trans. Fun. Mater. 131 (5) (2011) 389–394.
[2] P. Baudouin, A. Belhadj, F. Breaban, A. Deffontaine, Y. Houbaert, Effects of laser and mechanical cutting modes on the magnetic properties of low and medium si content nonoriented electrical steels, IEEE Trans. Magn. 38 (5) (2002) 3213–3215.
[3] D.J.B. Smith, B.C. Mecrow, G.J. Atkinson, A.G. Jack, A.A.A. Mehna, Shear stress concentrations in permanent magnet rotor sleeves, in: Proc. Int. Conf. Electr. Mach., ICEM, Rome, Italy, 2010, pp. 1–6.
[4] M. Rekik, O. Hubert, L. Daniel, Influence of a multiaxial stress on the reversible and irreversible magnetic behaviour of 3% si-fe alloy, Int. J. Appl. Electromagn. Mech. 44 (3–4) (2014) 301–315.
[5] L. Bernard, L. Daniel, Effect of stress on magnetic hysteresis losses in a switched reluctance motor: application to stator and rotor shrink fitting, IEEE Trans. Magn.

51 (2015) 7002513.

[6] S. Zeze, Y. Kai, T. Todaka, M. Enokizono, Vector magnetic characteristic analysis of a pm motor considering residual stress distribution with complex-approximated material modelling, IEEE Trans. Magn. 48 (11) (2012) 3352–3355.

[7] K. Yamazaki, Y. Kato, Iron loss analysis of interior permanent magnet synchronous motors by considering mechanical stress and deformation of stators and rotors, IEEE Trans. Magn. 50 (2) (2014) 7022504.

[8] D. Miyagi, N. Maeda, Y. Ozeki, K. Miki, N. Takashi, Estimation of iron loss in motor core with shrink fitting using fem analysis, IEEE Trans. Magn. 45 (3) (2009) 1704–1707.

[9] V. Permiakov, L. Dupre, D. Makaveev, J. Melkebeek, Dependence of power losses on tensile stress for fe-si nonoriented steel up to destruction, J. Appl. Phys. 91 (10) (2002) 7854–7856.

[10] V. Permiakov, L. Dupre, A. Pulnikov, J. Melkebek, Loss separation and parameters for hysteresis modelling under compressive and tensile stresses, J. Magn. Magn. Mater. 272–276 (2004) e553–e554.

[11] D. Singh, P. Rasilo, F. Martin, A. Belahcen, A. Arkkio, Effect of mechanical stress on excess loss of electrical steel sheets, IEEE Trans. Magn. 51 (11) (2015) 1001204.

[12] J. Karthaus, S. Steentjes, N. Leuning, K. Hameyer, Effect of mechanical stress on different iron loss components up to high frequencies and magnetic flux densities, Int. J. Comp. Math. 36 (2017) 580–592.

[13] K. Ali, K. Atallah, D. Howe, Prediction of mechanical stress effects on the iron loss in electrical machines, J. Appl. Phys. 81 (1997) 4119–4121.

[14] H. Naumoski, A. Maucher, U. Herr, Investigation of the influence of global stresses and strains on the magnetic properties of electrical steels with varying alloying

content and grain size, in: 5th Int. Elc. Dri. Prod. Conf. (EDPC), 2015, pp. 1–8.

[15] G. Bertotti, General properties of power losses in soft ferromagnetic materials, IEEE Trans. Magn. 24 (1) (1988) 621–630.

[16] Y. Kai, M. Enokizono, Y. Kido, Measurement of vector magnetic properties of nonoriented electrical steel sheet under shear stress, Elc. Eng. Jpn. 191 (2015) 1–7.

[17] Y. Kai, M. Enokizono, Y. Kido, Influence of shear stress on vector magnetic properties on non-oriented electrical steel sheets, Int. J. Appl. Electromagn. Mech. 44 (3–4) (2014) 371–378.

[18] Y. Kai, M. Enokizono, Effect of arbitrary shear stress on vector magnetic properties of non-oriented electrical steel sheets, IEEE Trans. Magn. 53 (11) (2017) 2002304.

[19] K. Yamazaki, H. Mukaiyama, L. Daniel, Effect of multi-axial mechanical stress on loss characteristics of electrical steel sheets and interior permanent magnet machines, IEEE Trans. Magn. 54 (3) (2018) 1300304.

[20] U. Aydin, P. Rasilo, F. Martin, A. Belahcen, L. Daniel, A. Haavisto, A. Arkkio, Effect of multi-axial stress on iron losses of electrical steel sheets, J. Magn. Magn. Mater. 469 (2019) 19–27.

[21] U. Aydin, F. Martin, P. Rasilo, A. Belahcen, A. Haavisto, D. Singh, L. Daniel, A. Arkkio, Rotational single sheet tester for multiaxial magneto-mechanical effects in steel sheets, IEEE Trans. Magn. 55 (3) (2019) 2001810.

[22] A. Pulnikov, Modification of magnetic properties of non oriented electrical steels by the production of electromagnetic devices (Ph.D. thesis), Ghent University, Ghent/ Belgium, 2004.

[23] U. Aydin, P. Rasilo, F. Martin, D. Singh, L. Daniel, A. Belahcen, M. Rekik, O. Hubert, R. Kouhia, A. Arkkio, Magneto-mechanical modeling of electrical steel sheets, J. Magn. Magn. Mater. 439 (2017) 82–90.